



Comprehensive Modeling of Vehicle Air Conditioning Loads Using Heat Balance Method

2013-01-1507

Published
04/08/2013

Mohammad Ali Fayazbakhsh and Majid Bahrami
Simon Fraser University

Copyright © 2013 SAE International

doi:10.4271/2013-01-1507

ABSTRACT

The Heat Balance Method (HBM) is used for estimating the heating and cooling loads encountered in a vehicle cabin. A load estimation model is proposed as a comprehensive standalone model which uses the cabin geometry and material properties as the inputs. The model is implemented in a computer code applicable to arbitrary driving conditions. Using a lumped-body approach for the cabin, the present model is capable of estimating the thermal loads for the simulation period in real-time.

Typical materials and a simplified geometry of a specific hybrid electric vehicle are considered for parametric studies. Two different driving and ambient conditions are simulated to find the contribution and importance of each of the thermal load categories. The Supplemental Federal Test Procedure (SFTP) standard driving cycle is implemented in the simulations for two North American cities and the results are compared. It is concluded that a predictive algorithm can be devised according to the driving conditions, vehicle speed, orientation, and geographical location. By using this model, the pattern of upcoming changes in the comfort level can be predicted in real-time in order to intelligently reduce the overall AC power consumption while maintaining driver thermal comfort.

INTRODUCTION

Efficient design of mobile air conditioning (AC) has been the center of attention of automotive manufacturers and academic researchers during the last few decades. Reduction of fuel consumption and tailpipe emission are two crucial targets for the auto industry. Air conditioning operation is proven to have a significant impact on the emissions and fuel economy; e.g. AC usage can increase NO_x emission from 15% to 100% [1]. The AC power consumption of mid-size cars is estimated

to be higher than 12% of the total vehicle power during regular commuting [2]. AC is a critical system for hybrid electric vehicles (HEVs) and electric vehicles (EVs), as it is the second most energy consuming system after the electric motor [3]. Further, AC loads are the most significant auxiliary loads present in conventional ICE vehicles today; its energy use even outweighs the energy loss to rolling resistance, aerodynamic drag, or driveline losses for a typical vehicle. The U.S. alone consumes about 7 billion gallons of fuel a year for AC systems of light-duty vehicles [4]. The AC load of a 1200-kg sedan, under peak conditions, can amount to 6 kW, which can deplete the vehicle's battery pack quickly. Farrington *et al.* [3] investigated opportunities to reduce AC loads in EVs and HEVs. They reported that the driving range of EV can be reduced by nearly 40% due to AC usage. Welstand *et al.* [1] also studied the effects of AC on vehicle emissions and fuel consumption. Besides emission and fuel efficiency, passengers' comfort is another major factor that should be considered in the design of new vehicles. In fact, auto manufacturers pay a significant attention to driver and passenger comfort which is directly linked to AC system. This trend is evidenced by new features such as multi-zone climate control and heated/cooled seats that can be found even in recent compact vehicles. Based on these observations, it is of both environmental and economic interest to seek new methods to improve the efficiency and performance of AC systems of vehicle.

A clear understanding of the heating and cooling loads, encountered by the passenger cabin, is a key prerequisite for an efficient design of any mobile AC system. The function of AC system is to compensate for the continuous changes of cabin loads in order to maintain the passenger comfort within a thermal 'comfort zone'. Fanger's model of thermal comfort [5] has been extensively used in AC research and applications as the basis for comfort assessment. Based on Fanger's model, Ingersoll *et al.* [6] developed a human thermal

comfort calculation model specific to automobile passenger cabins. While performing thermal load calculations for a vehicle cabin, their model can be used to assess the corresponding status of thermal comfort.

ASHRAE Handbook of Fundamentals [7] provides two major thermal load calculation methodologies: Heat Balance Method (HBM) and Weighting Factor Method (WFM). HBM is the most scientifically rigorous available method and can consider more details with less simplifying assumptions [8]. An advantage of HBM is that several fundamental models can be incorporated in the thermal calculations. Although HBM is more accurate than WFM, it is easier to implement WFM for load calculation in a passenger vehicle [8]. However, when more detailed information of the vehicle body and thermal loads is available, HBM is the preferred choice. Table 1 summarizes a number of previous studies on the estimation of thermal loads in vehicle cabins.

Table 1. Thermal load estimation models.

Study	Notes
Pedersen <i>et al.</i> [9]	A basic form of HBM application proposed. Method tested on a simple geometry.
Zheng <i>et al.</i> [10]	Ambient, radiation, ventilation, and metabolic loads considered.
Arici <i>et al.</i> [11]	Analytical solution combined with cooling cycle model.
Ding and Zito [12]	Analytical solution for cabin temperature with ambient load.
Selow <i>et al.</i> [13]	System-level modeling of a vehicle performed.
Alexandrov <i>et al.</i> [14]	Computational fluid dynamics simulation of cabin air distribution.
Khayyam <i>et al.</i> [15]	Design of an energy management system based on thermal load estimations performed.

Recently, Zheng *et al.* [10] devised a simple method to calculate vehicle's thermal loads. They calculated the different loads such as the radiation and ambient loads. A case study was performed and the results were validated using wind tunnel climate control tests. The different loads were separately calculated and summed up to give the total heat gain or loss from the cabin. Arici *et al.* [11] developed a computer code for simulating the dynamic operation of a climate control system for a typical vehicle. They considered the transition of both the cabin temperature and the relative humidity as predicted by the principles of heat and mass transfer; a lumped system model was developed. The components of the AC system were also simulated to work

alongside the thermal load balance equations. Ding and Zito [12] also used a lumped model for the cabin and solved the corresponding transient heat transfer differential equation analytically. Their analytical solution can be used as a benchmark for basic problems like the cool-down test. Selow *et al.* [13] developed a virtual vehicle based on experimental correlations for each significant vehicle component. The virtual vehicle was divided into different modules one of which was the cabin climate. Such simultaneous operation of these modules could provide estimations without necessitating cumbersome and costly experiments.

Besides experimental tests, numerical simulations have also been used to improve the understanding of AC load estimations. Methods put forth by ASHRAE and other bodies often assume the cabin as a "lumped system" and do not take the three-dimensional distribution of temperature and flow parameters into account. Finding exact solutions for distribution of air flow, temperature, humidity, etc. is often complex, thus numerical methods have been employed for such simulations. Alexandrov *et al.* [14] used two- and three-dimensional CFD simulations to investigate the effect of various parameters such as car velocity and outside temperature on the performance of mobile AC systems. They simulated the flow in a typical vehicle and found a maximum temperature difference of about 7°C between two points in the car cabin. They concluded that issues such as low air circulation zones in the cabin can be resolved by designing better air inlet and outlet configurations.

The goal of cooling and heating load estimations is to provide thermal comfort for passengers efficiently. To do this, it is necessary to control the AC cycle to maintain the air quality within the desirable limits specified by a comfort model. Khayyam *et al.* [15] collected a set of models to calculate the different types of thermal loads encountered in a vehicle. These models were later used to estimate the overall cooling load which was fed to a coordinated energy management system to reduce the air conditioning energy consumption [16]. In conventional AC systems, where the compressor is run by energy supplied from the engine, improvement of the AC system is inseparable from the overall vehicle fuel consumption. Khayyam *et al.* [17] used similar models to combine with a fuzzy logic air conditioning enhanced look-ahead system which estimated future road slope within a distance ahead of the vehicle. They showed that 12% energy consumption savings can be achieved using their proposed enhanced fuzzy system. Wei and Dage [18] developed an intelligent cabin climate control system based on human-sensory response to comfort factors. They used passive remote infrared sensors to measure passenger skin temperatures. An intelligent climate controller then controlled the parameters such as the blower speed to provide passenger thermal comfort.

The Heat Balance Method (HBM) allows continuous improvement of load calculation models through applying empirical models and correlations [19]. The essence of this method is the conservation of mass and thermal energy. Because of this approach, much geometrical and thermal detail should be known before applying it to a specific enclosure. This makes HBM an intensive method which is avoided in some engineering applications. On the other hand, due to the fundamental approach of HBM, knowing more details can improve the accuracy of HBM models.

This paper aims to provide a new and comprehensive model for estimating thermal loads in vehicle cabins. Although other load estimation models exist as mentioned above, the main emphasis of this study is to account for the dynamic changes to the AC loads that occur in real-world scenarios. The results of this study can be used by HVAC engineers to design more efficient mobile AC systems. A specifically calibrated model for any vehicle can be later implemented to provide accurate predictions of upcoming thermal load variations under various driving and environmental conditions. As such, the ultimate objective of this study is to create a platform for real-time control of the AC system, including AC compressor, heat exchanger fans, passenger(s) seat temperature and window glazing, to achieve superior fuel efficiency and passenger comfort.

MODEL DEVELOPMENT

We consider a lumped model of a typical vehicle cabin. The net heat gain by the cabin can be classified under nine different categories. The total load as well as each of these loads can either be positive (heating up the cabin) or negative (cooling down the cabin) and may depend on various driving parameters. In the following, the models developed for each of these load categories are presented and discussed. Some of the correlations used in the present model are based on experiments performed on certain vehicles, which are used here for general validation of the model. New correlations can be readily plugged into the present model can be tailored to any new vehicle, after specifying those correlations for the case.

The summation of all the load types will be the instantaneous cabin overall heat load gain. The mathematical formulation of the model can thus be summarized as

$$\begin{aligned} \dot{Q}_{Tot} = & \dot{Q}_{Met} + \dot{Q}_{Dir} + \dot{Q}_{Dif} + \dot{Q}_{Ref} + \\ & \dot{Q}_{Amb} + \dot{Q}_{Exh} + \dot{Q}_{Eng} + \dot{Q}_{Ven} + \\ & \dot{Q}_{AC} \end{aligned} \quad (1)$$

All of the above \dot{Q} values are thermal energies per unit time. \dot{Q}_{Tot} is the net overall thermal load encountered by the cabin. \dot{Q}_{Met} is the metabolic load. \dot{Q}_{Dir} , \dot{Q}_{Dif} , and \dot{Q}_{Ref} are the direct,

diffuse, and reflected radiation loads, respectively. \dot{Q}_{Amb} is the ambient load. \dot{Q}_{Exh} and \dot{Q}_{Eng} are the exhaust and engine loads due to the high temperature of the exhaust gases and the engine. Finally, the term \dot{Q}_{Ven} is the load generated due to ventilation, and \dot{Q}_{AC} is the thermal load created by the AC cycle.

Figure 1 schematically shows the various thermal load categories encountered in a typical vehicle cabin. Some of the above loads pass across the vehicle body plates/parts, while others are independent of the surface elements of the cabin.

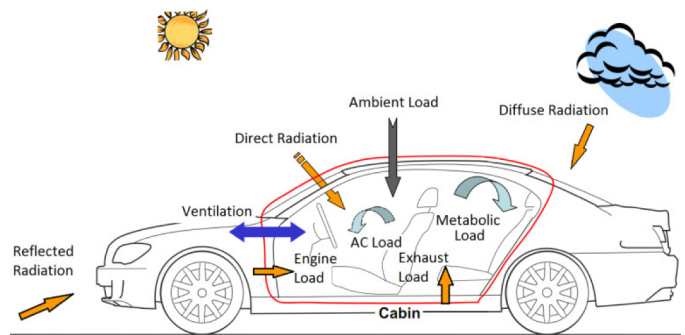


Figure 1. Schematic representation of thermal loads in a typical vehicle cabin.

Each thermal load is calculated assuming a quasi-steady-state condition. Load calculations are performed at time steps during the simulation period of interest, and after every time step, all the load components are algebraically summed up and the new cabin air temperature and surface element temperatures are calculated as

$$\begin{aligned} \Delta T_i &= \frac{\dot{Q}_{Tot}}{m_a c_a + DTM} \Delta t \\ \Delta T_s &= \frac{\dot{Q}_s}{m_s c_s} \Delta t \end{aligned} \quad (2)$$

where ΔT_i and ΔT_s are the change in the cabin and surface element temperatures at the current time step. DTM is the sum of all the deep thermal masses *i.e.* the overall thermal inertia of all objects other than air present inside the cabin. These objects include the seat structures, the dash, the dash components, etc. which are combined with the cabin air in the lumped model. Δt is the time step, m_a is the cabin air mass and c_a is the air specific heat. m_s and c_s are the mass and specific heat of each of the surface elements and $\dot{Q}_s = \dot{Q}_{s,Rad} + \dot{Q}_{s,Amb}$ is the net heat gain by a surface element consisting of the heat gain by radiation, $\dot{Q}_{s,Rad}$, and the heat gain from ambient, $\dot{Q}_{s,Amb}$.

Metabolic Load

The metabolic activities inside human body constantly create heat and humidity (*i.e.* perspiration). This heat passes through the body tissues and is finally released to the cabin air. This amount is considered as a heat gain by the cabin air and is called the metabolic load. The metabolic load can be calculated by

$$\dot{Q}_{Met} = \sum_{Passengers} MA_{Du} \quad (3)$$

where M is the passenger metabolic heat production rate. It is found from the tabulated values in ISO 8996 [20] based on various criteria such as occupation and activity levels. For a driver and a sitting passenger, the values can be estimated as 85 W/m^2 and 55 W/m^2 , respectively. The DuBois area A_{Du} , which is an estimation of the body surface area as a function of height and weight, is calculated by [20]

$$A_{Du} = 0.202W^{0.425}H^{0.725} \quad (4)$$

where W and H are the passenger weight and height, respectively.

Radiation Load

The heat gain due to solar radiation is a significant part of the cooling loads encountered in vehicles. According to ASHRAE [7], solar radiation heat load can be categorized into direct, diffuse, and reflected radiation loads.

Direct radiation is that part of the incident solar radiation which directly strikes a surface of the vehicle body, which is calculated from

$$\dot{Q}_{Dir} = \sum_{Surfaces} S\tau i_{Dir} \cos \theta \quad (5)$$

where i_{Dir} is the direct radiation heat gain per unit area and θ is the angle between the surface normal and the position of sun in the sky. τ is the surface element transmissivity and S is the surface area, respectively. Before local sunrise and after local sunset, simply no radiation loads are considered. The direct radiation heat gain per unit area is found by

$$i_{Dir} = \frac{A}{\exp\left(\frac{B}{\sin \beta}\right)} \quad (6)$$

where A and B are constants tabulated in ASHRAE Handbook of Fundamentals [7] for different months. β is the altitude angle that is calculated based on position and time.

Diffuse radiation is the part of solar radiation which results from indirect radiation of daylight on the surface. During a

cloudy day, most of the solar radiation is received from this diffuse radiation. The diffuse radiation heat gain is found by

$$\dot{Q}_{Dif} = \sum_{Surfaces} S\tau i_{Dif} \quad (7)$$

Similarly, i_{Dif} is the diffuse radiation heat gain per unit area which is calculated from

$$i_{Dif} = Ci_{Dir} \frac{1 + \cos \Sigma}{2} \quad (8)$$

where Σ is the surface tilt angle measured from the horizontal surface and the values for C are tabulated in [7].

Reflected radiation refers to the part of radiation heat gain that is reflected from the ground and strikes the body surfaces of the vehicle. The reflected radiation is calculated by

$$\dot{Q}_{Ref} = \sum_{Surfaces} S\tau i_{Ref} \quad (9)$$

i_{Ref} , the reflected radiation heat gain per unit area, is calculated from

$$i_{Ref} = (i_{Dir} + i_{Dif}) \rho_g \frac{1 - \cos \Sigma}{2} \quad (10)$$

where ρ_g is the ground reflectivity coefficient. Based on the absorptivity of each particular surface element, a percentage of the incident radiation load can be absorbed by that surface, hence increasing its temperature. The net absorbed heat of each surface element due to radiation can thus be written as

$$\dot{Q}_{s.Rad} = S\alpha (i_{Dir} \cos \theta + i_{Dif} + i_{Ref}) \quad (11)$$

where α is the surface absorptivity.

Ambient Load

The ambient load is the contribution of the thermal load transferred to the cabin air due to temperature difference between the ambient and cabin air. Exterior convection, conduction through body panels, and interior convection are involved in the total heat transfer between the ambient and the cabin. Equation (12) shows the general form of the ambient load model.

$$\dot{Q}_{Amb} = \sum_{Surfaces} SU(T_s - T_i) \quad (12)$$

where U is the overall heat transfer coefficient of the surface element. T_s and T_i are the average surface temperature and average cabin temperature, respectively. U has different

components consisting of the inside convection, conduction through the surface, and outside convection. It can be written in the form

$$U = \frac{1}{R} \quad \text{where} \quad R = \frac{1}{h_o} + \frac{\lambda}{k} + \frac{1}{h_i} \quad (13)$$

where R is the net thermal resistance for a unit surface area. h_o and h_i are the outside and inside convection coefficients, k is the surface thermal conductivity, and λ is the thickness of the surface element. The thermal conductivity and thickness of the vehicle surface can be measured rather easily. The convection coefficients h_o and h_i depend on the orientation of the surface and the air velocity. Here, the following estimation is used to estimate the convection heat transfer coefficients as a function of vehicle speed [21]

$$h = 0.6 + 6.64\sqrt{V} \quad (14)$$

where h is the convection heat transfer coefficient in W/m^2K and V is the vehicle speed in m/s . Despite its simplicity, this correlation is applicable in all practical automotive instances [21]. The cabin air is assumed stationary and the ambient air velocity is considered equal to the vehicle velocity. Numerical simulations can also be used to provide the model with convection coefficients that have higher accuracy and take into account the different orientation and position of every surface component.

Similar to the radiation load above, a portion of the ambient load across the body surface is absorbed by the body plate material. The heat gain or loss of each surface element is the difference between the heat gained from the ambient by the surface, and the heat released to the cabin by the surface. Thus we can write the net absorbed heat as

$$\begin{aligned} \dot{Q}_{s,Amb} &= SU(T_o - T_s) - SU(T_s - T_i) \\ &= SU(T_o - 2T_s + T_i) \end{aligned} \quad (15)$$

where T_o , T_i , and T_s are the ambient, cabin, and surface average temperatures, respectively.

Exhaust Load

Conventional and hybrid electric vehicles have an Internal Combustion Engine (ICE) that creates exhaust gases. The Exhaust Gas Temperature (EGT) can reach as high as $1000^\circ C$ [22]. Because of the high temperature of the exhaust gas, some of its heat can be transferred to the cabin through the cabin floor. Considering S_{Exh} as the area of the bottom surface in contact with the exhaust pipe, the exhaust heat load entering the cabin can be written as

$$\dot{Q}_{Exh} = S_{Exh} U (T_{Exh} - T_i) \quad (16)$$

where U is the overall heat transfer coefficient of the surface element in contact with the exhaust pipe and it should be calculated by Eq. (13) assuming no external convection since the exhaust temperature is measured at the outer side of the bottom surface. S_{Exh} is the surface area exposed to the exhaust pipe temperature and T_{Exh} is the exhaust gas temperature. The temperature of the exhaust gases in Celsius degrees is estimated by [15]

$$T_{Exh} = 0.138RPM - 17 \quad (17)$$

where RPM is the engine speed in revolutions per minute.

Engine Load

Similar to the exhaust load above, the high temperature engine of a conventional or hybrid car can also contribute to the thermal gain of the cabin. Equation (18) shows the formulation used for calculating the engine thermal load.

$$\dot{Q}_{Eng} = S_{Eng} U (T_{Eng} - T_i) \quad (18)$$

where U is the overall heat transfer coefficient of the surface element in contact with the engine and S_{Eng} is the surface area exposed to the engine temperature. The overall heat transfer coefficient can be calculated by Eq. (13) assuming no external convection, since the engine temperature is measured at the outside of the front surface. T_{Eng} is the engine temperature and is estimated in Celsius degrees by [15]

$$T_{Eng} = -2 \times 10^{-6} RPM^2 + 0.0355RPM + 77.5 \quad (19)$$

Ventilation Load

Fresh air is allowed to enter the vehicle cabin to maintain the air quality for passengers. As the passengers breathe, the amount of CO_2 concentration linearly increases over time. Thus, a minimum flow of fresh air should be supplied into the cabin to maintain the passengers comfort. Arndt and Sauer [23] reported the minimum fresh air requirements for different numbers of passengers in a typical vehicle. For instance, a minimum of 13% fresh air is needed for a single passenger.

On the other hand, Fletcher and Saunders [24] reported the air leakage from different vehicle types. They showed that for typical vehicles, leakage occurs as a function of the pressure difference between the cabin and the surroundings as well as the vehicle velocity. For a small sedan car at a pressure difference of $10 Pa$, a leakage of $0.02 m^3/s$ was reported [24].

Because of the air conditioning and ventilation, the cabin pressure is normally slightly higher than the ambient. Thus, the ventilation load has to take the leakage air flow rate into account. Meanwhile, in the steady-state operation, the built-

up pressure is assumed to remain constant. Hence, ambient air is assumed to enter the cabin at the ambient temperature and relative humidity, and the same flow rate is assumed to leave the cabin at the cabin temperature and relative humidity.

According to psychrometric calculations, ventilation heat gain consists of both sensible and latent loads. To account for both these terms, assuming a known flow rate of fresh air entering the cabin, the amount of thermal heat gain can be calculated from

$$\dot{Q}_{Ven} = \dot{m}_{Ven} (e_o - e_i) \quad (20)$$

where \dot{m}_{Ven} is the ventilation mass flow rate and e_o and e_i are the ambient and cabin enthalpies, respectively. Enthalpies are calculated from [25]

$$e = 1006T + (2.501 \times 10^6 + 1770T)X \quad (21)$$

where T is air temperature and X is humidity ratio in gram of water per gram of dry air. Humidity ratio is calculated as a function of relative humidity by

$$X = 0.62198 \frac{\phi P_s}{100P - \phi P_s} \quad (22)$$

where ϕ is relative humidity, P is air pressure, and P_s is the water saturation pressure at temperature T .

AC Load

The duty of the air conditioning system is to compensate for other thermal loads so that the cabin temperature remains within the acceptable comfort range. In cold weather conditions, positive AC load (heating) is required for the cabin. Inversely, in warm conditions, negative AC load (cooling) is needed for maintaining the comfort conditions. The actual load created by the AC system depends on the system parameters and working conditions. In this work, it is assumed that an AC (or heat pump) cycle is providing the thermal load calculated by

$$\dot{Q}_{AC} = - \left(\begin{array}{l} \dot{Q}_{Met} + \dot{Q}_{Dir} + \dot{Q}_{Dif} + \dot{Q}_{Ref} + \\ \dot{Q}_{Amb} + \dot{Q}_{Exh} + \dot{Q}_{Eng} + \dot{Q}_{Ven} \end{array} \right) - (m_a c_a + DTM)(T_i - T_{comf}) / t_c \quad (23)$$

T_{comf} is the target comfort temperature as described and widely used by ASHARE standards [7]. This is the target bulk cabin temperature which is assumed comfortable at the conditions under consideration. t_c is a pull-down constant which determines the overall pull-down time. Pull-down time is defined as the time required for the cabin temperature to

reach the comfort temperature within 1 K. Using Eq. (23) for the air conditioning load, the pull-down constant can be calculated from

$$t_c = \frac{t_p}{\ln |T_0 - T_{comf}|} \quad (24)$$

where T_0 is the initial cabin temperature.

Of course, the actual AC load depends on the system sizing and design. For a given system, the load may change depending on the compressor and fan speed as well. The actual power consumption of the cycle should be estimated by considering a suitable Coefficient of Performance (COP) for the vapor compression cycle. Equation (23) is used in this study as a guideline for analyzing the performance of an AC system in a typical vehicle. It shows that analyzing different scenarios with the AC cycle can help efficient sizing and control of the air conditioning cycle.

CABIN GEOMETRY

In order to perform the energy simulations of the present model, the geometry of the cabin should be known. Often the compartment geometry is available in a 3D modeling software. In this study, we used the Polygon File Format (PLY) for importing geometry into the present model. This format stores the 3D surface data in a flexible and portable file which can be of ASCII structure [26]. The format is originally designed to store 3D data achieved from 3D scanners. Thus, in case of scanning the cabin interior area for an energy analysis, the PLY format will be a convenient way of easily plugging the geometry into the code. Also, many broadly-used 3D modeling tools support the PLY format directly.

In the present 3D model, the surfaces are stored in memory as triangles where material and geometrical properties are stored. Figure 2 shows the triangulation of a sample cabin surface. Every triangle element contains all the required material and geometrical properties assigned to that surface. Geometrical properties such as the area and the direction of the normal to the surface are calculated in the code as well. In case of the lumped energy simulation of the cabin, the whole inside air can be abstracted as a single node. On the other hand, the 3D geometry contains various surface triangles which provide a means of heat transfer to and from the ambient. In this study, all of the incoming and outgoing heat loads are assumed to contribute to the heat gain of the lumped body. The energy simulation modules can be coupled to the present numerical simulation codes in order to extend the comprehensive model to a 3D energy simulation model.

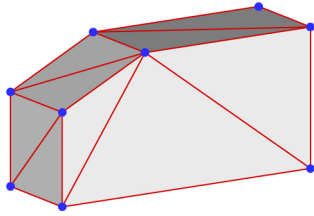


Figure 2. Schematic of the triangulation of vehicle surface elements for storing material and geometrical properties.

RESULTS AND DISCUSSION

The model is implemented in an object-oriented computer program using the C++ language. The simulation model is flexible and can be used for different cabin geometries, driving scenarios, and ambient conditions. An important part of thermal load estimations is the underlying database used for cabin geometry, materials, weather conditions, driving cycles/duties, etc. In the present simulations, a simplified version of the cabin of eVaro, shown in Fig. 3, is used for the dimensions. The eVaro is a hybrid electric vehicle designed and built by Future Vehicle Technologies [27]. The eVaro has one driver and one passenger seat which are positioned in tandem. Figure 4 shows the simplified geometry and dimensions of the cabin, as used for simulations in this work.

Table 2 summarizes the properties assigned to different surfaces of the body. Surfaces 1 and 2 are assumed to be glass with 3 mm thickness, while the other surfaces are taken to be a typical vehicle body with 10 mm thickness. 10% of surface number 5 (front) is subject to the engine temperature, while 1% of surface number 4 (bottom) is assumed to be subject to the exhaust temperature.



Figure 3. A picture of eVaro hybrid electric vehicle by Future Vehicle Technologies [27].

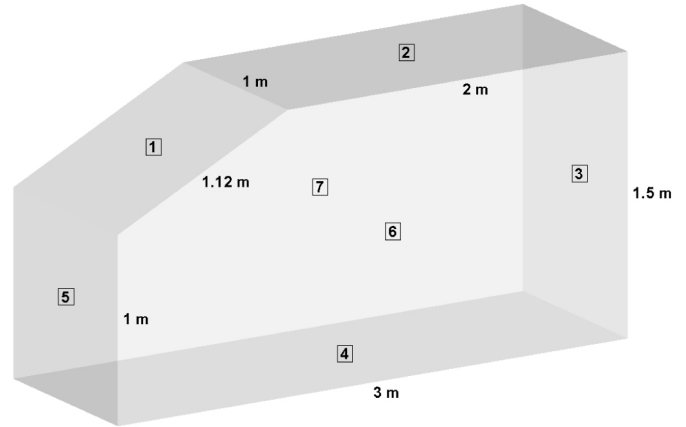


Figure 4. Schematic of the simulated cabin geometry.

Table 2. Properties of the vehicle cabin body.

Property	Glass	Vehicle Body
Conductivity (W/mK)	1.05	0.2
Density (kg/m^3)	2500	1500
Transmissivity	0.5	0
Absorptivity	0.3	0.4
Specific Heat (J/kgK)	840	1000
Thickness (mm)	3	10

There are a number of standard driving cycles used in the auto industry as the basis for tests and analyses. Among many, the Supplemental Federal Test Procedure (SFTP) or the US06 driving cycle [28] was used as an example in this study. The driving cycle lasts 593 seconds; hence it is repeated consecutively to cover longer driving ranges for simulation time. Based on the gear changing according to the torque imposed on the wheels, the RPM values were estimated accordingly. Figure 5 shows the plot of the US06 driving cycle with the corresponding RPM values considered in this work.

Two different driving conditions are simulated using the above-mentioned geometry and material properties. In both cases, the consecutively-repeated US06 driving cycle was used and actual weather data were collected and used for the specific date and time under consideration. The sky condition has been reported as mainly clear for both simulations. In real-time application of the model, the actual weather conditions can be obtained via wireless connection and a Global Positioning System (GPS) to determine more accurate results. In the following, the input parameters are shown for both cases.

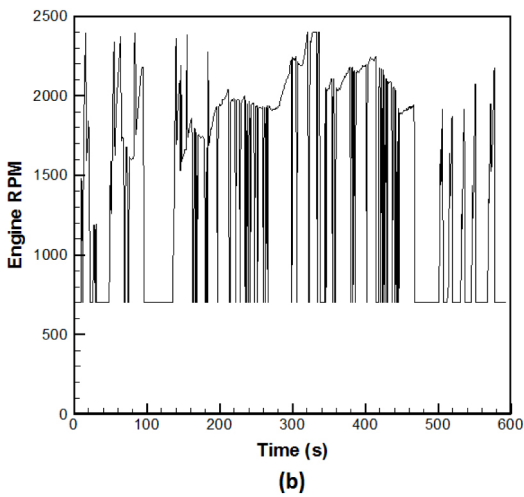
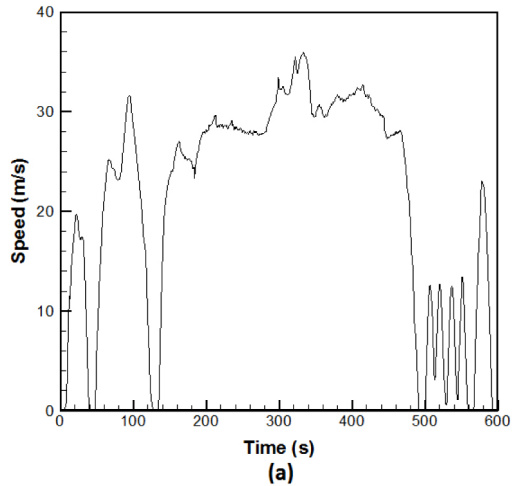


Figure 5. (a) US06 driving cycle (b) Estimated variation of engine RPM based on the US06 driving cycle.

Table 3. Specifications for the first simulated driving condition.

Specification	Value
Date	July 21, 2012
Local Time	13:00 to 16:00
Location	Houston, Texas
Driver Height, Weight	1.7 m, 70 kg
Passenger Height, Weight	1.6 m, 55 kg
Ventilation Flow	0.01 m ³ /s (21.2 CFM)
Ground Reflectivity	0.2
Ambient Temperature	34.4°C
Initial Cabin Temperature	80°C
Ambient Relative Humidity	70%
Cabin Relative Humidity	50%
Comfort Temperature	23°C
Pull-Down Time	600 s
Deep Thermal Mass	5600 J/K

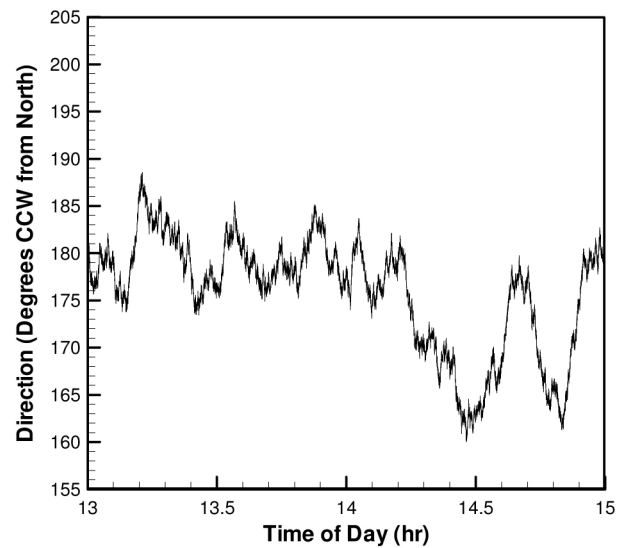


Figure 6. Driving direction for the first simulated driving condition, Houston, Texas, July 21, 2012, 13:00 to 16:00.

Driving Scenario 1

The specifications of the first driving condition are shown in Table 3. It is not efficient to use hot ambient air for ventilation when cooling is required. Therefore, a small amount of ventilation flow rate is assumed to account for the minimum fresh air requirements based on recommendations in [23] as well as the previously-mentioned leakages calculated according to [24]. It should also be noted that this is an arbitrary scenario considered in this study to investigate the ventilation load. Realistically, the passenger has the freedom to change the ventilation rate.

The initial cabin temperature was selected at 80°C in this driving condition. This is because the soaked interior temperatures can reach very high values for a vehicle with closed windows parked under solar radiation.

The vehicle is assumed to be driving approximately towards south. Figure 6 shows the random direction changes of the vehicle during the simulation time.

Figure 7 shows the variation of cabin air temperature with time. The net heat gain in the cabin has been plotted as well. Negative heat values mean heat loss from the cabin, while positive values mean heat gains by the cabin. Figure 7 shows that the cabin temperature decreases from a soak temperature of 80°C to the comfort temperature after almost 10 minutes represented by the pull-down time. According to ASHRAE Standard 55 [29], the comfort level of the cabin temperature is within the range of 22°C to 24°C and the comfort range of relative humidity is between 40% and 60%. Thus, the comfort temperature and cabin relative humidity are assumed to be 23°C and 50%, respectively. The cabin and ambient relative humidity values are assumed constant during the simulation period.

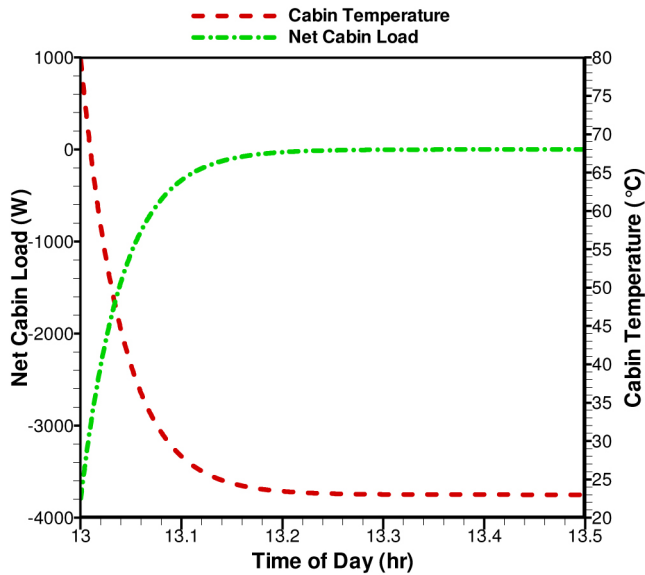


Figure 7. Net cabin load and cabin temperature for the first half hour of the first simulated driving condition, Houston, Texas, July 21, 2012. The values remain constant after the comfort level is reached.

Without using AC, high cabin temperature is anticipated because of the small cabin volume, high metabolic heat generation, high radiation, and hot ambient conditions. During the pull-down period, the AC system consumes more power and imposes a negative load on the cabin air to decrease the temperature to 23°C. After the pull-down, a steady-state situation is achieved where the loads are balanced and a zero net load is maintained for the cabin for the rest of the simulation period.

Figure 8 shows the contribution of each load category in the net thermal load gained by the cabin. It can be seen that the engine, exhaust, and reflected radiation loads are negligible. We can conclude that when seeking guidelines for reducing cabin heat gains in this driving condition, the engine, exhaust, and reflected radiation loads may be neglected from consideration. Khayyam *et al.* [16] also concluded that since proper insulation is used in most vehicles, the heat load from the engine and exhaust can be neglected in some scenarios. In such cases, the driving cycle will have an insignificant effect on the overall load estimation inside the cabin.

The direct and diffuse radiation loads, on the other hand, are important AC loads that tend to give rise to the cabin temperature. It is observed that the direct radiation load decreases due to the decrease in the sun elevation angle for the simulation period which is happening after midday. Metabolic load is another positive load which is constant due to no change in the number of passengers. Ventilation and ambient loads are functions of the temperature difference between cabin and ambient. During the first 5 minutes of simulation, the cabin temperature is higher than the ambient. It results in the negative starting values of these loads. After

the cabin temperature reaches the steady condition, the warmer ambient imposes almost constant positive ventilation and ambient loads.

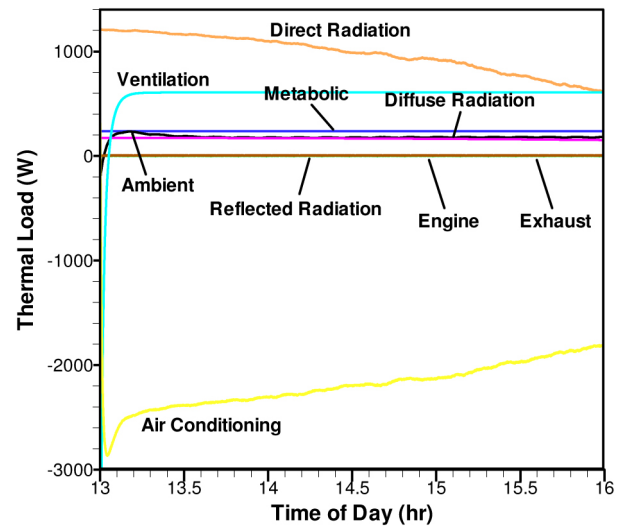


Figure 8. Comparison of thermal loads for the first simulated driving condition.

The assumed AC load formula of Eq. (23) reaches a peak absolute value of about 3000W at the beginning of the scenario. After this time, the pull-down of the cabin temperature finishes and the AC load reaches a balance with the rest of the loads. Then, the absolute AC load value gradually decreases since no more pull-down is required and the contribution of the direct radiation load as a positive heat gain is decreasing as well.

Stegou-Sagia *et al.* [30] showed that there is room for saving AC energy in residential areas by using carefully selected glazing material. For a vehicle cabin, a predictive algorithm can be implemented in the vehicle AC controller to calculate the loads in real-time. When the thermal loads are being estimated, the decision to decrease glazing transmissivity can be made and the cabin can be cooled down intelligently by keeping the radiation load from entering the cabin.

Figure 9 shows the advantage of using glazing transmissivity control on the vehicle glass. The same driving condition is assumed, but with different glass transmissivity constants. Figure 9 reveals that by decreasing transmissivity from 0.8 to 0.5, the required AC power consumption can be reduced by up to 30%. This shows that, in a hot and sunny ambient condition, much of the AC fuel consumption can be saved by using an intelligent glazing system. In a cold and sunny weather condition where the cabin should be heated up, the radiation from the sun actually helps the AC loads. In that case, AC controller should intelligently decide to increase glazing transmissivity, so the heating energy consumption is minimized by taking advantage of the free energy from solar radiation.

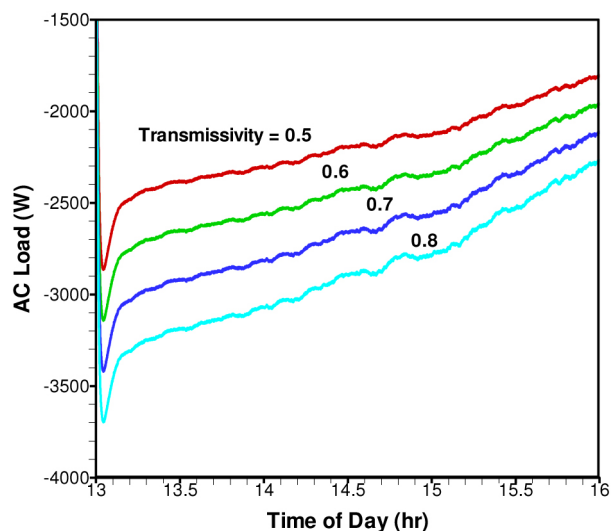


Figure 9. AC load for maintaining comfort in the first simulated driving condition with different glazing transmissivity values.

Driving Scenario 2

Table 4 lists the specifications of the second driving condition considered in this study. Also in this scenario, it is not suitable to use cold ambient air for ventilation when heating is required. A small ventilation flow rate is thus assumed to supply the minimum fresh air requirement and leakages identified in the ventilation load model described above.

Table 4. Specifications for the second simulated driving condition.

Specification	Value
Date	January 8, 2012
Local Time	4:00 to 7:00
Location	Toronto, Ontario
Driver Height, Weight	1.8 m, 76 kg
Passenger Height, Weight	No Passenger
Ventilation Flow	0.01 m ³ /s (21.2 CFM)
Ground Reflectivity	0.2
Ambient Temperature	-3.5°C
Initial Cabin Temperature	3°C
Ambient Relative Humidity	85%
Cabin Relative Humidity	60%
Comfort Temperature	23°C
Pull-Down Time	600 s
Deep Thermal Mass	5600 J/K

The vehicle is assumed to be driving approximately towards east, while Fig. 10 shows the random change of the vehicle direction used as the simulation input. Figure 11 shows the variation of the cabin air temperature and net cabin load for

driving condition 2. In this driving condition, the initial cabin temperature is below the comfort level of 23°C. In this cold scenario, a positive net cabin load is provided to the cabin in order to increase its temperature up to the comfort level. After 10 minutes, the net heat load becomes zero which means a balance between the AC heat load and the rest of the loads. After that time, the cabin temperature is maintained at the comfort level.

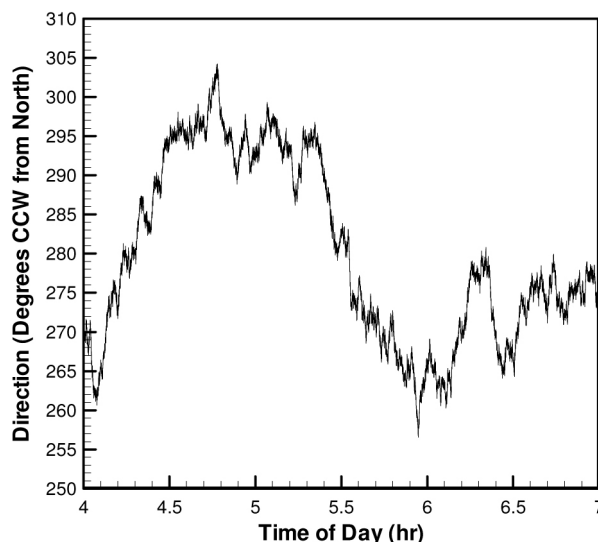


Figure 10. Net cabin load and cabin temperature for the first half hour of the first simulated driving condition, Toronto, Ontario, January 8, 2012, 04:00 to 07:00.

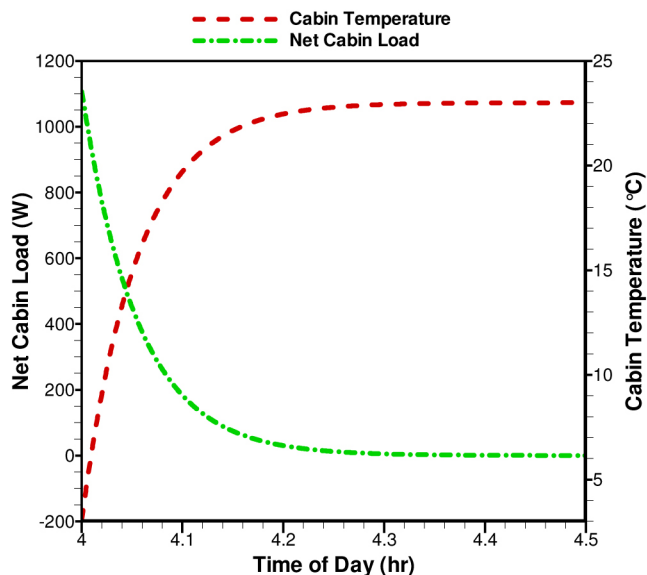


Figure 11. Net cabin load and cabin temperature for the first half hour of the second simulated driving condition, Toronto, Ontario, January 8, 2012. The values remain constant after the comfort level is reached.

Figure 12 compares the contribution of each load categories during the simulation. Again, negative and positive loads mean cabin heat losses and gains, respectively. In this driving condition, the simulation period is before the local sunrise and thus, there is no contribution by the direct, diffuse, or reflected radiations. Also, the engine and exhaust loads are negligible as discussed in the first driving condition.

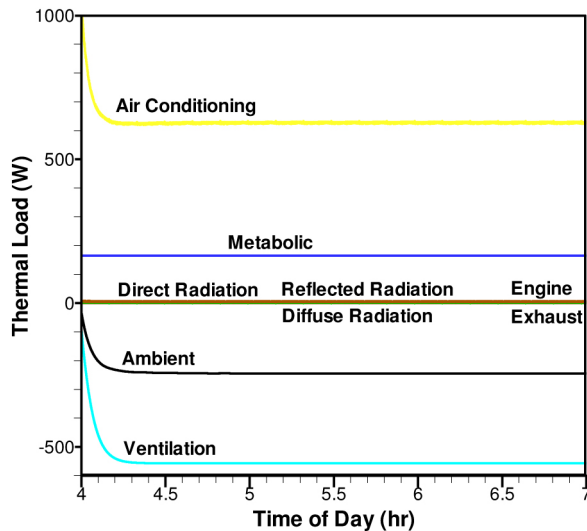


Figure 12. Comparison of thermal loads for the second simulated driving condition.

Due to the cold ambient temperature of this scenario, the ventilation and ambient loads have negative contributions to the cabin loads. This means that the cabin is losing heat to the ambient through these mechanisms. The positive metabolic load is not able to provide enough heat to keep the cabin temperature at the comfort level. Thus, a positive AC load of about 600 W has been required to maintain the comfort level.

As observed here, ventilation is causing a heat loss of more than 500 W from the cabin in the cold condition. This is definitely undesirable in terms of thermal comfort, but may be unavoidable due to leakages or fresh air requirements.

SUMMARY AND CONCLUSIONS

Mobile air conditioning systems should be designed to compensate for the continuous changes of the cabin thermal loads in order to maintain passenger thermal comfort. In this paper, the Heat Balance Method (HBM) is applied to a vehicle cabin to model the various heating and cooling loads transferred to the cabin via radiation, convection, or conduction. Mathematical models of heat transfer phenomena are used to calculate the different load categories.

A comprehensive heat balance model is developed for usage in mobile air conditioning design. A new comprehensive AC design tool is developed. Mathematical load calculation models are devised and collected from various sources to

create a comprehensive stand-alone model of load estimation. Quasi-steady-state and lumped-body assumptions are made and a constant time-stepping is performed by the computer simulation code. After every time step, the total heat gain (or heat loss) by the cabin air increases (or decreases) the cabin air temperature accordingly. Cabin wall temperatures are updated after each time step as well.

The present computer simulation takes the vehicle geometry, material properties, and driving condition characteristics as input. By incorporating future study results from numerical simulations or experimental tests, the correlations inside the model can be upgraded. For example, the heat transfer coefficient on every part of the cabin surface can be correlated from simulations conducted specifically on a certain vehicle in order to gain reliable results.

To perform case studies, specific material properties and the simplified geometry of a hybrid electric vehicle are considered in this paper. Two different scenarios are simulated to find the contribution of each of the load categories. A standard driving cycle is applied in the simulations for two different North American cities and the results are compared.

Simulations of different driving scenarios show that some load categories such as the engine, exhaust, and reflected radiation are often negligible, while others such as the ambient or ventilation load can play important roles in the variation of cabin temperature.

For real-life cases, an intelligent algorithm can be devised using the present model. By implementing this algorithm in the car computer, the pattern of upcoming changes can be predicted and accommodated in the AC load in real-time. The necessary modifications in the controllable features of the car such as the glazing transmissivity and the ventilation flow rate can be performed intelligently to provide the comfort level while maintaining energy efficiency.

REFERENCES

1. Welstand, J., Haskew, H., Gunst, R., and Bevilacqua, O., "Evaluation of the Effects of Air Conditioning Operation and Associated Environmental Conditions on Vehicle Emissions and Fuel Economy," SAE Technical Paper 2003-01-2247, 2003, doi:10.4271/2003-01-2247.
2. Lambert, M. A., and Jones, B. J., "Automotive Adsorption Air Conditioner Powered by Exhaust Heat. Part 1: Conceptual and Embodiment Design," Proceedings of the Institution of Mechanical Engineers, Part D: Journal of Automobile Engineering, 220(7):959-972, 2006, doi: 10.1243/09544070JAUTO221.
3. Farrington, R., Cuddy, M., Keyser, M., and Rugh, J., "Opportunities to Reduce Air-Conditioning Loads Through

Lower Cabin Soak Temperatures,” Presented at the 16th Electric Vehicle Symposium, China, October 13-16, 1999.

4. Johnson, V., “Fuel Used for Vehicle Air Conditioning: A State-by-State Thermal Comfort-Based Approach,” SAE Technical Paper [2002-01-1957](#), 2002, doi: [10.4271/2002-01-1957](#).

5. Fanger, P. O., “Thermal Comfort: Analysis and Applications in Environmental Engineering,” McGraw-Hill, New York, 1972.

6. Ingersoll, J., Kalman, T., Maxwell, L., and Niemiec, R., “Automobile Passenger Compartment Thermal Comfort Model - Part II: Human Thermal Comfort Calculation,” SAE Technical Paper [920266](#), 1992, doi: [10.4271/920266](#).

7. ASHRAE Handbook of Fundamental, American Society of Heating, Refrigerating, and Air Conditioning, Atlanta, GA, 1988.

8. Kamar, H., Senawi, M., and Kamsah, N., “Computerized Simulation of Automotive Air-Conditioning System: Development of Mathematical Model and Its Validation,” International Journal of Computer Science Issues, 9(2):23-34, 2012.

9. Pedersen, C. O., Fisher, D. E., and Liesen, R. J., “Development of a Heat Balance Procedure for Calculating Cooling Loads,” ASHRAE Transactions, 103(2):459-468, 1997.

10. Zheng, Y., Mark, B., and Youmans, H., “A Simple Method to Calculate Vehicle Heat Load,” SAE Technical Paper [2011-01-0127](#), 2011, doi: [10.4271/2011-01-0127](#).

11. Arici, O., Yang, S., Huang, D., and Oker, E., “Computer Model for Automobile Climate Control System Simulation and Application,” International Journal of Applied Thermodynamics, 2(2):59-68, 1999.

12. Ding, Y. and Zito, R., “Cabin Heat Transfer and Air Conditioning Capacity,” SAE Technical Paper [2001-01-0284](#), 2001, doi: [10.4271/2001-01-0284](#).

13. Selow, J., Wallis, M., Zoz, S., and Wiseman, M., “Towards a Virtual Vehicle for Thermal Analysis,” SAE Technical Paper [971841](#), 1997, doi: [10.4271/971841](#).

14. Alexandrov, A., Kudriavtsev, V., and Reggio, M., “Analysis of Flow Patterns and Heat Transfer in Generic Passenger Car Mini-Environment,” Presented at 9th Annual Conference of the CFD Society of Canada, Canada, May 27-29, 2001.

15. Khayyam, H., Kouzani, A. Z., and Hu, E. J., “Reducing Energy Consumption of Vehicle Air Conditioning System by an Energy Management System,” Presented in IEEE The 4th International Green Energy Conference, China, 2009.

16. Khayyam, H., Kouzani, A. Z., Hu, E. J., and Nahavandi, S., “Coordinated Energy Management of Vehicle Air Conditioning System,” Applied Thermal Engineering, 31(5): 750-764, 2011, doi: [10.1016/j.applthermaleng.2010.10.022](#).

17. Khayyam, H., Nahavandi, S., Hu, E., Kouzani, A., Chonka, A., Abawajy, J., Marano, V., and Davis, S., “Intelligent Energy Management Control of Vehicle Air Conditioning via Look-Ahead System,” Applied Thermal Engineering, 31(16):3147-3160, 2011, doi: [10.1016/j.applthermaleng.2011.05.023](#).

18. Wei, K. C., and Dage, G. A., “An Intelligent Automotive Climate Control System,” IEEE International Conference on Systems, Man and Cybernetics. Intelligent Systems for the 21st Century, 4:2977-2982, 1995, doi: [10.1109/ICSMC.1995.538237](#).

19. Barnaby, C. S., Spitler, J. D., and Xiao, D., “The Residential Heat Balance Method for Heating and Cooling Load Calculations,” ASHRAE Transactions, 111(1):308-319, 2005.

20. ISO Standard, “Ergonomics of the Thermal Environment - Determination of Metabolic Heat Production,” ISO Standard 8996, Rev. 2004.

21. Ingersoll, J., Kalman, T., Maxwell, L., and Niemiec, R., “Automobile Passenger Compartment Thermal Comfort Model - Part I: Compartment Cool-Down/Warm-Up Calculation,” SAE Technical Paper [920265](#), 1992, doi: [10.4271/920265](#).

22. Talbi, M., and Agnew, B., “Energy Recovery from Diesel Engine Exhaust Gases for Performance Enhancement and Air Conditioning,” Applied Thermal Engineering, 1(5): 5-10, 2002.

23. Arndt, M., and Sauer, M., “Spectroscopic Carbon Dioxide Sensor for Automotive Applications,” Sensors, Proceedings of IEEE 2004, 1:252-255, 2004.

24. Fletcher, B., and Saunders, C., “Air Change Rates in Stationary and Moving Motor Vehicles,” Journal of Hazardous Materials, 38:243-256, 1994.

25. Singh, A. K., Singh, H., Singh, S. P., and Sawhney, R. L., “Numerical Calculation of Psychrometric Properties on a Calculator,” Building and Environment, 37(4):415-419, 2002, doi: [10.1016/S0360-1323\(01\)00032-4](#).

26. McHenry, K., and Bajcsy, P., “An Overview of 3D Data Content, File Formats and Viewers,” National Center for Supercomputing Applications, 1205 W Clark, Urbana, IL 61801, Technical Report ISDA08-002, 2008.

27. Future Vehicle Technologies, <http://www.futurevehicletechnologies.com>, October 2012.

28. United States Environmental Protection Agency, <http://www.epa.gov>, October 2012.

29. ASHRAE Standard, “Thermal Environmental Conditions for Human Occupancy,” ASHRAE Standard 55, Rev. 2012.

30. Stegou-Sagia, A., Antonopoulos, K., Angelopoulou, C., and Kotsiovelos, G., “The Impact of Glazing on Energy Consumption and Comfort,” Energy Conversion and

Management, 48(11):2844-2852, 2007. doi: [10.1016/j.enconman.2007.07.005](https://doi.org/10.1016/j.enconman.2007.07.005).

CONTACT INFORMATION

Mohammad Ali Fayazbakhsh
PhD Candidate, Mechatronic Systems Engineering
School of Engineering Science
Simon Fraser University, Surrey, BC V3T 0A3, Canada
mfayazba@sfu.ca

Dr. Majid Bahrami, P.Eng.
Associate Professor, Mechatronic Systems Engineering
School of Engineering Science
Simon Fraser University, Surrey, BC V3T 0A3, Canada
mbahrami@sfu.ca

ACKNOWLEDGMENTS

This work was supported by Automotive Partnership Canada (APC), Grant No. APCPJ 401826-10. The authors would like to thank the technical support of the industry partner of the project, Future Vehicle Technologies Inc. (Maple Ridge, British Columbia, Canada).

NOMENCLATURES

A - Apparent Solar Irradiation at Air Mass = 0 (W/m^2)

A_{Du} - DuBois Body Surface Area (m^2)

B - Atmospheric Extinction Coefficient

c - Specific Heat ($J/kg K$)

C - Diffuse Radiation Factor

DTM - Deep Thermal Mass (J/K)

e - Enthalpy (J/kg)

h - Convective Heat Transfer Coefficient (W/m^2K)

H - Human Body Height (m)

I - Radiation Heat Gain per Unit Area (W/m^2)

k - Conductive Heat Transfer Coefficient (W/mK)

m - Mass (kg)

m - Mass Flow Rate (kg/s)

M - Metabolic Rate (W/m^2)

P - Air Pressure (Pa)

P_s - Water Saturation Pressure (Pa)

Q - Cooling/Heating Load (W)

R - Surface Overall Heat Transfer Resistance (m^2K/W)

RPM - Engine Revolutions per Minute ($1/min$)

S - Cabin Surface Element Area (m^2)

t_c - Pull-Down Constant (s)

t_p - Pull-Down Time (s)

T - Temperature (K)

T₀ - Initial Cabin Temperature (K)

U - Surface Overall Heat Transfer Coefficient (W/m^2K)

V - Vehicle Speed (m/s)

V̇ - Ventilation Flow Rate (m^3/s)

W - Human Body Weight (kg)

X - Humidity Ratio ($kg\ water/kg\ dry\ air$)

Greek Letters

α - Absorptivity

β - Altitude Angle ($^\circ$)

Δt - Time Step Size (s)

ΔT - Temperature Change (K)

φ - Relative Humidity (%)

λ - Surface Element Thickness (m)

θ - Angle between Surface Normal and Sun Position ($^\circ$)

ρ - Density (kg/m^3)

ρ_g - Ground Reflectivity

Σ - Surface Tilt Angle from Horizon ($^\circ$)

τ - Transmissivity

Subscripts

a - Cabin Air

AC - Air Conditioning

Amb - Ambient

comf - Comfort Condition

Dif - Diffuse Radiation

Dir - Direct Radiation

Eng - Engine

Exh - Exhaust

i - Inside

Met - Metabolic

new - New Time Step

o - Outside

old - Old Time Step

Rad - Radiation

Ref - Reflected Radiation

s - Surface Element

Tot - Total

Ven - Ventilation

The Engineering Meetings Board has approved this paper for publication. It has successfully completed SAE's peer review process under the supervision of the session organizer. This process requires a minimum of three (3) reviews by industry experts.

All rights reserved. No part of this publication may be reproduced, stored in a retrieval system, or transmitted, in any form or by any means, electronic, mechanical, photocopying, recording, or otherwise, without the prior written permission of SAE.

ISSN 0148-7191

Positions and opinions advanced in this paper are those of the author(s) and not necessarily those of SAE. The author is solely responsible for the content of the paper.

SAE Customer Service:

Tel: 877-606-7323 (inside USA and Canada)

Tel: 724-776-4970 (outside USA)

Fax: 724-776-0790

Email: CustomerService@sae.org

SAE Web Address: <http://www.sae.org>

Printed in USA